

CORRECTION

Open Access



Correction to: EIF4A3-induced circular RNA MMP9 (circMMP9) acts as a sponge of miR-124 and promotes glioblastoma multiforme cell tumorigenesis

Renjie Wang^{1,2}, Sai Zhang^{1,2}, Xuyi Chen^{1,2}, Nan Li^{1,2}, Jianwei Li^{1,2}, Ruichao Jia^{1,2}, Yuanqing Pan³ and Haiqian Liang^{1,2,4*}

Correction to: *Mol Cancer* 17, 166 (2018)
<https://doi.org/10.1186/s12943-018-0911-0>

Following the publication of the original article [1], authors found out that it contains a duplication error within Figs. 4h and 5b. The correct version of Figs. 4 and 5 are shown below. In addition, the correct version of Fig. 1 and Additional file 1 are also provided in this paper.

Published online: 30 October 2020

Reference

1. Wang R, Zhang S, Chen X, et al. EIF4A3-induced circular RNA MMP9 (circMMP9) acts as a sponge of miR-124 and promotes glioblastoma multiforme cell tumorigenesis. *Mol Cancer*. 2018;17:166. <https://doi.org/10.1186/s12943-018-0911-0>.

Supplementary information

Supplementary information accompanies this paper at <https://doi.org/10.1186/s12943-020-01271-w>.

Additional file 1 : Table S1. The primers used in this study

Author details

¹Institute of Traumatic Brain Injury and Neurology, Characteristic Medical Center of Chinese People's Armed Police Force, Tianjin 300162, China. ²Department of Neurosurgery, Characteristic Medical Center of Chinese People's Armed Police Force, Tianjin 300162, China. ³Department of Basic Medicine, Tianjin Medical College, Tianjin 300222, China. ⁴Chinese Glioma Cooperative Group (CGCG), Tianjin, China.

The original article can be found online at <https://doi.org/10.1186/s12943-018-0911-0>.

* Correspondence: lianghaiqian711@163.com

¹Institute of Traumatic Brain Injury and Neurology, Characteristic Medical Center of Chinese People's Armed Police Force, Tianjin 300162, China
²Department of Neurosurgery, Characteristic Medical Center of Chinese People's Armed Police Force, Tianjin 300162, China
Full list of author information is available at the end of the article



© The Author(s). 2020 **Open Access** This article is licensed under a Creative Commons Attribution 4.0 International License, which permits use, sharing, adaptation, distribution and reproduction in any medium or format, as long as you give appropriate credit to the original author(s) and the source, provide a link to the Creative Commons licence, and indicate if changes were made. The images or other third party material in this article are included in the article's Creative Commons licence, unless indicated otherwise in a credit line to the material. If material is not included in the article's Creative Commons licence and your intended use is not permitted by statutory regulation or exceeds the permitted use, you will need to obtain permission directly from the copyright holder. To view a copy of this licence, visit <http://creativecommons.org/licenses/by/4.0/>. The Creative Commons Public Domain Dedication waiver (<http://creativecommons.org/publicdomain/zero/1.0/>) applies to the data made available in this article, unless otherwise stated in a credit line to the data.

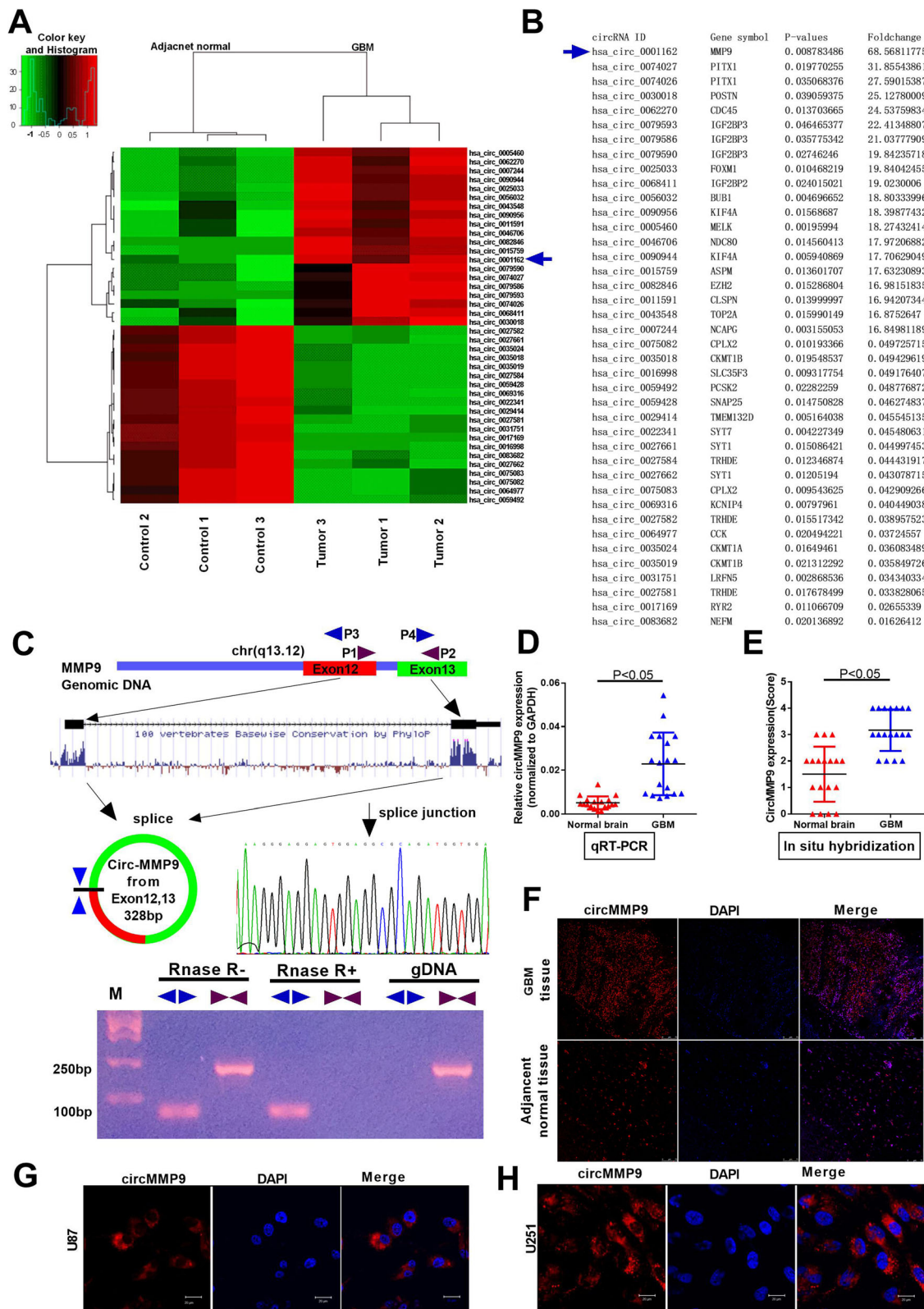
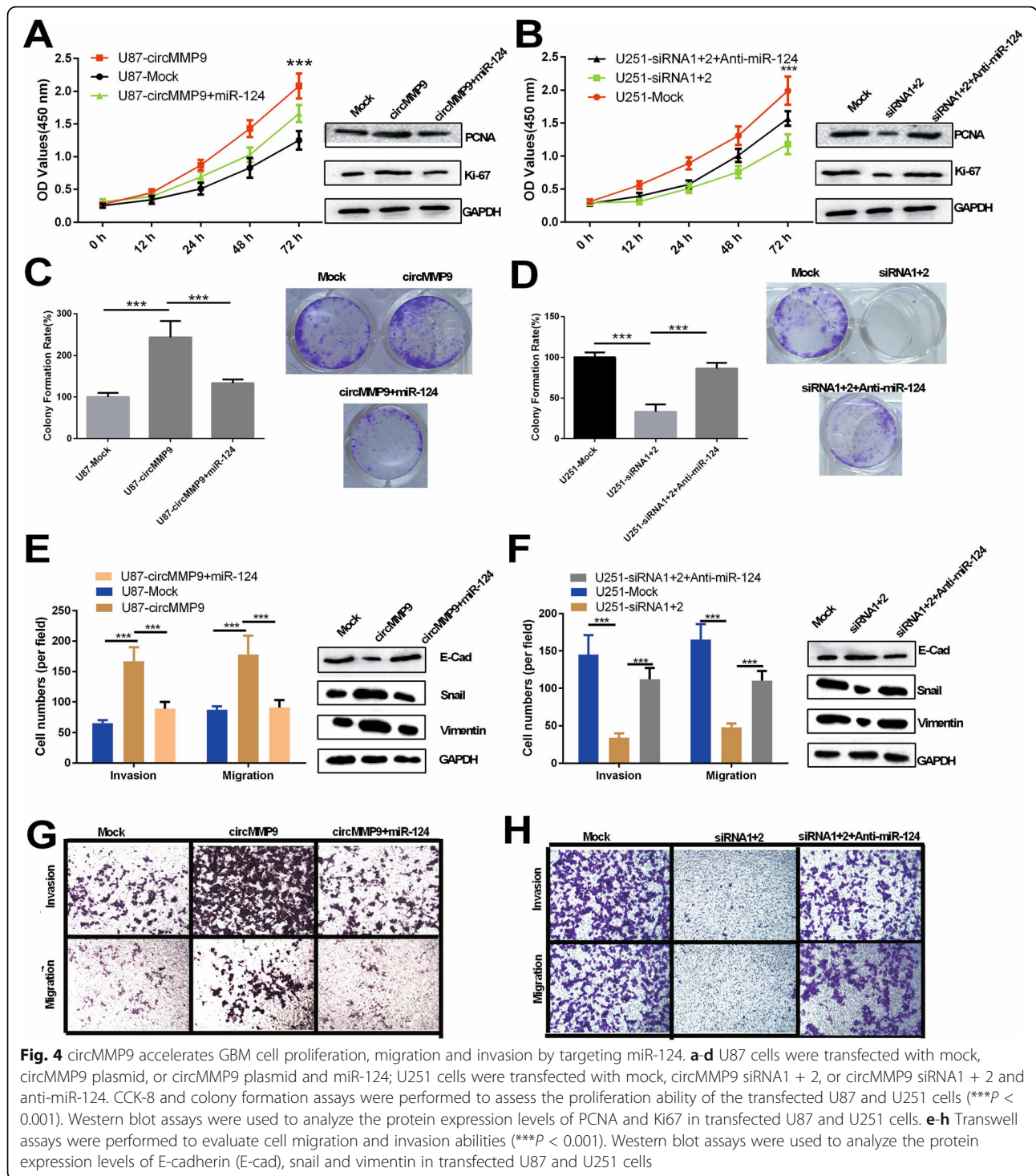


Fig. 1. (See legend on next page.)

(See figure on previous page.)

Fig. 1. Characterization of circMMP9 in human GBM. **a** Clustered heat map showing tissue-specific circRNAs (top 20 upregulated and downregulated circRNAs), which are displayed on a scale from green (low) to red (high), between three human GBM tissues and adjacent normal tissues. The arrow represents the circRNA (hsa_circ_001162) with the greatest differential expression. **b** Detailed information for the top 20 upregulated and downregulated circRNAs according to the extent. **c** Schematic representation of circMMP9 formation. The splice junction sequence was Sanger sequenced, and the RNAs were detected via PCR. Divergent primers could produce circRNAs in cDNA but not in genomic DNA (gDNA); convergent primers could produce cDNA and gDNA. **d** The expression level of circMMP9 was detected by qRT-PCR in GBM tissues and adjacent normal brain tissues ($n = 18$, $P < 0.05$); GAPDH served as the internal control. **e-f** circMMP9 expression was measured using in situ hybridization (FISH) in GBM tissues and adjacent normal brain tissues ($n = 18$, $P < 0.05$). **g-h** Confocal FISH was performed to determine the location of circMMP9 in U87 and U251 cells



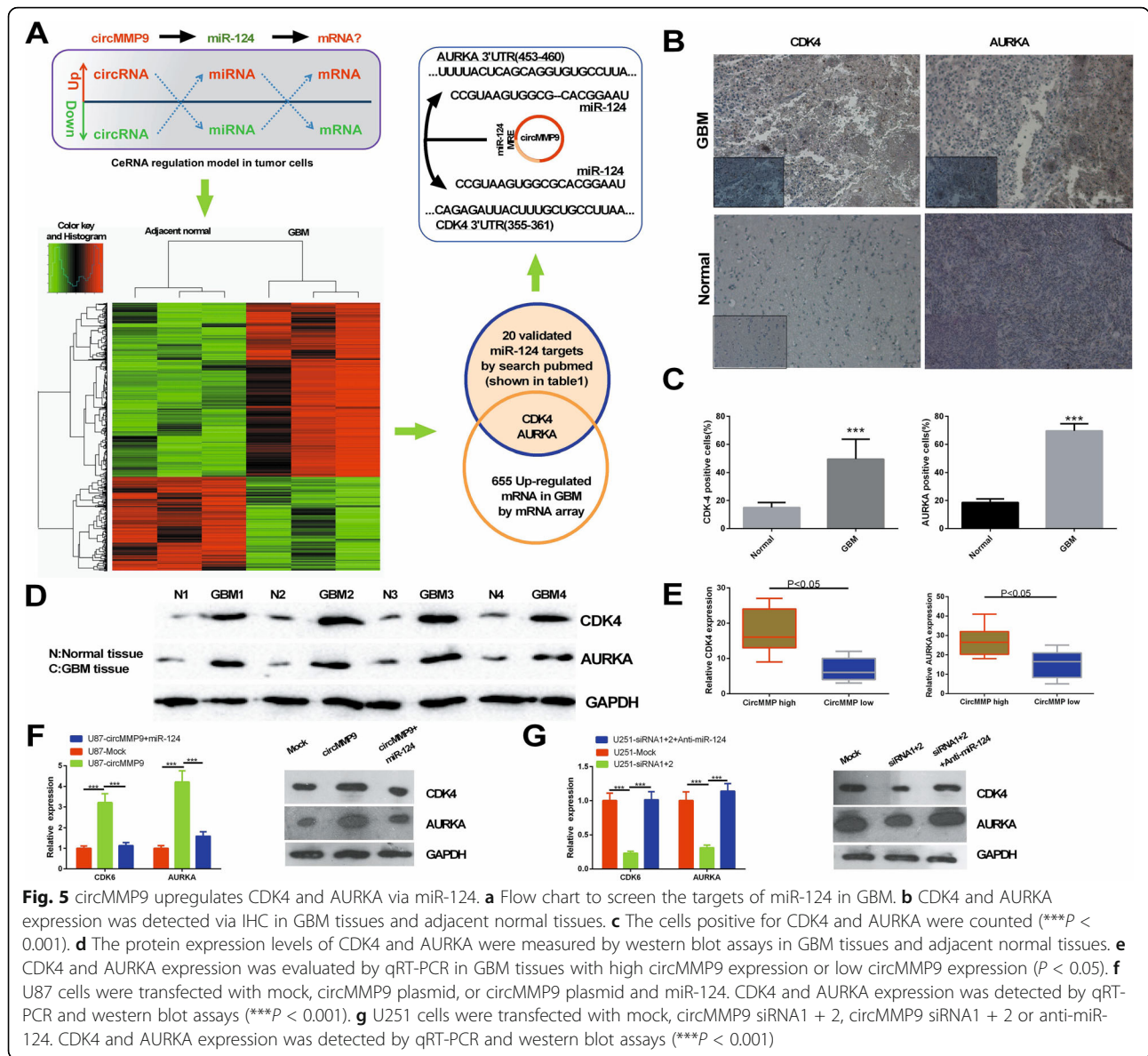


Fig. 5 circMMP9 upregulates CDK4 and AURKA via miR-124. **a** Flow chart to screen the targets of miR-124 in GBM. **b** CDK4 and AURKA expression was detected via IHC in GBM tissues and adjacent normal tissues. **c** The cells positive for CDK4 and AURKA were counted ($***P < 0.001$). **d** The protein expression levels of CDK4 and AURKA were measured by western blot assays in GBM tissues and adjacent normal tissues. **e** CDK4 and AURKA expression was evaluated by qRT-PCR in GBM tissues with high circMMP9 expression or low circMMP9 expression ($P < 0.05$). **f** U87 cells were transfected with mock, circMMP9 plasmid, or circMMP9 plasmid and miR-124. CDK4 and AURKA expression was detected by qRT-PCR and western blot assays ($***P < 0.001$). **g** U251 cells were transfected with mock, circMMP9 siRNA1 + 2, circMMP9 siRNA1 + 2 or anti-miR-124. CDK4 and AURKA expression was detected by qRT-PCR and western blot assays ($***P < 0.001$)